ARTICLES

Intramolecular and Low-Frequency Intermolecular Vibrations of Pentacene Polymorphs as a Function of Temperature

Raffaele Guido Della Valle,* Elisabetta Venuti, Luca Farina, and Aldo Brillante

Dipartimento di Chimica Fisica e Inorganica and INSTM-UdR Bologna, Università di Bologna, Viale Risorgimento 4, I-40136 Bologna, Italy

Matteo Masino and Alberto Girlando

Dipartimento di Chimica G.I.A.F. and INSTM-UdR Parma, Università di Parma, Parco Area delle Scienze, I-43100, Parma, Italy

Received: May 26, 2003

Single crystals of pentacene with different morphologies (polymorphs **C** and **H**) have been studied by Raman spectroscopy as a function of temperature from 79 to 300 K. All Raman active lattice modes and a range of low-frequency intramolecular modes have been identified and assigned. The experiments are compared with quasi harmonic lattice dynamics (QHLD) calculations of the crystallographic structures and vibrational frequencies as a function of temperature. Experiments and calculations both indicate that the two polymorphs are stable over a wide temperature range.

Introduction

The polymorphism of pentacene has been the subject of intense experimental[1−9] and theoretical[10,11] studies. Recently,[12,13] by analyzing the five complete X-ray structures published so far,[1−5] we noticed that they correspond to two different "inherent structures"[14] of mechanical equilibrium, i.e., to two local minima of the potential energy surface. This behavior indicates that there are at *least* two different single crystals polymorphs of pentacene.[12,13] One of the polymorphs, labeled as phase **C**, corresponds to the structure originally determined by Campbell et al.[1,2] The other polymorph, phase **H**, corresponds to the structure found in the more recent measurements.[3−5] In a later computational work[15] we obtained information on the *global* stability of the minima by systematically sampling the potential surface and found that the polymorphs **C** and **H** do correspond to the two deepest minima. Other deep minima with layered structures, which might correspond to the thin film polymorphs found to grow on substrates,[5−9] were also predicted. Although the calculations clearly indicate that *both* polymorphs are mechanically stable, one might still harbor doubts[5,10] about the existence of the form reported by Campbell et al.,[1,2] because all the recent X-ray studies have failed to reproduce it.[3−5,9] For this reason, it is important to stress that we have also reached conclusive *experimental* evidence[16,17] that polymorph **C** does exist. In fact, we have shown[16] that two different crystal morphologies can be obtained by changing the method of crystal growth. At room temperature the two forms present clearly distinguishable Raman spectra, closely matching those calculated[12,13,16] for polymorphs **C** and **H**. The two phases have also been recognized directly through X-ray experiments,[17] which indeed yield two distinct structures, matching the published measurements for forms **C**[1,2] and **H**.[3−5] Raman experiments as a function of pressure[17,18] also reveal that polymorph **C** transforms irreversibly into polymorph **H**, with a sluggish phase transition starting around 0.2 GPa.

In this paper we present Raman spectra as a function of temperature for the two different polymorphs. These measurements yield improved spectral resolution at low temperatures and allow us to investigate on the possible occurrence of a temperature-dependent phase transition similar to that observed under compression. The experimental temperature dependence of the frequencies is compared with the results of quasi harmonic lattice dynamics[19−21] (QHLD) calculations. These calculations allow us to describe the effects of temperature and to account for the coupling between lattice and intramolecular vibrations.

The paper is organized as follows. We first present the experimental methods and the Raman phonon spectra. We then discuss the computational methods and compare the results to the experimental data. Finally, we summarize the conclusions that can be drawn from this study.

Experimental Methods

Samples of pentacene, polymorph **H**, were directly selected from metal-like bluish platelets of commercial products (Koch & Light and Fluka purum). For polymorph **C**, we used instead tiny vapor-grown blue microcrystals obtained by fast sublimation in an atmosphere of about 4.0 kPa (40 mbar) of nitrogen at a temperature of 500 K. Raman spectra in the region of the lattice phonons and of the low-energy intramolecular modes were recorded with the spectrometer Jobin Yvon T64000. The laser power was kept low (about 50 mW) to prevent thermal damage of the sample. To avoid excitonic luminescence[22] from the

* To whom correspondence should be addressed. E-mail:valle@aronte.fci.unibo.it. WWW:http://www.fci.unibo.it/∼valle/.

10.1021/jp0354550 CCC: $27.50
Published on Web 01/17/2004

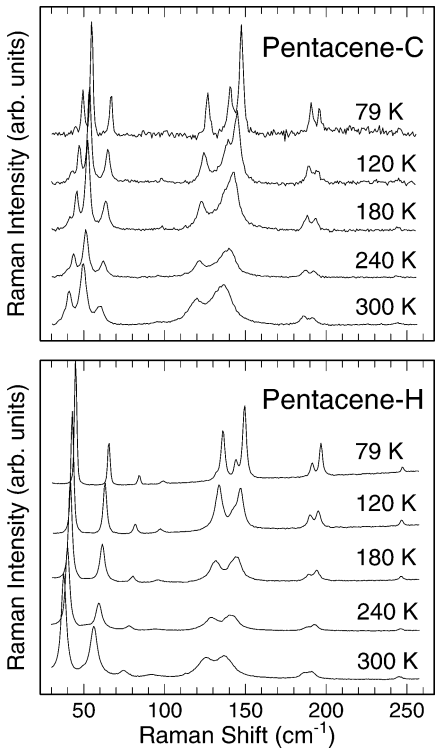

Figure 1. Raman spectra for polymorphs **C** and **H** of pentacene at selected temperatures.

sample, the Raman scattering has been recorded using low-energy excitation from a krypton laser tuned at 752.5 nm. Even in these conditions, the Raman spectra of polymorphs **C** below 120 K are partially overlapped by a smooth luminescence background that has been removed from the Raman spectra shown in Figure 1.

Low temperature spectra down to 79 K were recorded with a conventional cryostat (Linkam HFS 91) directly placed on the stage of the microscope (Olympus BX40) interfaced to the spectrometer. The use of a 20× magnification objective allowed us to reach a spatial resolution of about 2.4 μm, yielding the possibility to check the physical purity of crystal polymorphs by carefully probing the lattice phonon profiles within the sample surface.[16] The chemical purity of the crystals was checked by mass spectrometry, elemental analysis, and IR spectroscopy.

Raman Spectra

Raman spectra for phases **C** and **H** at selected temperatures are shown in Figure 1. The corresponding temperature dependence of the mode frequencies is displayed in Figure 2, together with the calculated dependence, which will be discussed below. We have observed the same temperature dependence by cooling to 79 K or by heating back toward room temperature T and found that all spectral changes are continuous and fully reversible. The Raman frequencies at 79 K are listed in Table 2.

Both phases **C**[1,2] and **H**[3−5] are triclinic and belong to the space group $P\bar{1}$ (C_i^1). The unit cell contains two independent molecules located on the (0, 0, 0) and ($^1/_2$, $^1/_2$, 0) inversion sites, giving rise to anthracene-like herringbone structures. The factor group analysis for the lattice phonons at $k = 0$ predicts six Raman active modes of A_g symmetry and three IR active modes of A_u symmetry. Because pentacene is a highly flexible molecule, we also expect a number of low-lying intramolecular doublets, each arising from a mode of the isolated molecule. As shown in the following, the distinction between lattice and intramolecular modes is not sharp because they strongly mix.

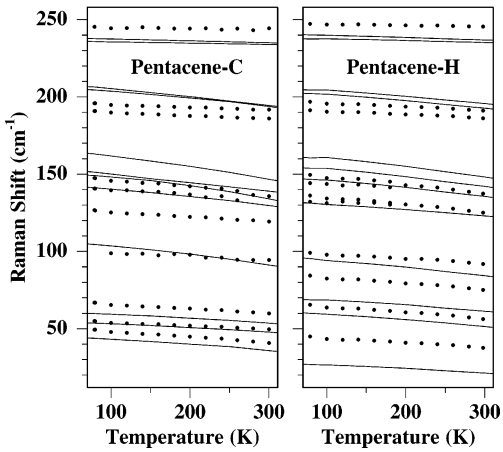

Figure 2. Phonon frequencies vs temperature for polymorphs **C** and **H** of pentacene. Symbols: Raman measurements. Lines: calculations for A_g phonons.

The experimental Raman frequencies of the lowest lattice modes (below 100 cm^{-1}) differ significantly between phases **H** and **C**. For phase **C** the three lowest lattice modes are clustered in a narrow frequency range around 55 cm^{-1}, and one very one weak mode is found near 100 cm^{-1} (Figure 1, upper panel). For phase **H**, instead, there are four lattice modes almost uniformly spread in the range 30−100 cm^{-1} (Figure 1, lower panel). The two other lattice modes, virtually coincident for the two polymorphs, lie around 140 cm^{-1}, where two bands are present at room temperature. These bands exhibit weak shoulders on the low-energy side, observable only at low temperatures and assigned to intramolecular vibrations. For both phases, all additional bands above 160 cm^{-1} are safely assigned to intramolecular vibrations.

Computational Methods

Following a well tested procedure for calculating crystal structures and vibrational frequencies,[23,24] we start from ab initio molecular geometry, atomic charges, vibrational frequencies, and Cartesian eigenvectors of the normal modes of the isolated pentacene molecule. These data were determined with the Gaussian98 program[25] (revision A.5), using the 6-31G(d) basis set combined with the B3LYP exchange correlation functional.[25,26] The frequencies, scaled by the factor of 0.9613 recommended for the combination of B3LYP and 6-31G(d),[27,28] agree satisfactorily with previous theoretical and experimental results.[29]

The ab initio molecular geometry was used to model the crystallographic structures. Starting separately from each of the five published X-ray structures,[1−5] we replaced the experimental molecular geometries with the ab initio one, and then minimized the total potential energy of the crystal Φ with respect to the lattice parameters, molecular positions, and orientations. For the intermolecular potential Φ we adopted an atom−atom Buckingham model,[30] with Williams parameter set IV,[31] combined with an electrostatic contribution represented by a set of ab initio atomic charges. Instead of the Mulliken charges, we have chosen the potential derived charges, which describe directly the electrostatic potential.[25] The convergence of the electrostatic interactions was accelerated by Ewald's method.[30]

After determining the structures of minimum potential energy Φ, which allowed us to confirm once again that there are two different phases, we accounted for the effects of temperature T and pressure p by calculating the structures of minimum Gibbs energy $G(p,T)$ with quasi harmonic lattice dynamics[19−21]

TABLE 1: Lattice Parameters of Pentacene[a]

	structure	T	a	b	c	α	β	γ	V
H	calc min Φ	−	5.930	7.614	14.793	79.104	85.320	85.590	652.42
	calc min G	90	5.955	7.664	14.838	79.163	85.073	85.598	661.39
	calc min G	180	5.964	7.697	14.915	79.071	84.838	85.723	668.33
	calc min G	293	5.986	7.776	14.949	79.448	84.168	85.707	679.43
	exp[5]	90	6.239	7.636	14.330	76.978	88.136	84.415	661.94
	exp[3]	180	6.275	7.714	14.442	76.752	88.011	84.524	677.32
	exp[5]	293	6.266	7.775	14.530	76.475	87.682	84.684	685.15
	exp[4]	293	6.265	7.786	14.511	76.65	87.50	84.61	685.50
	exp[17]	295	6.268	7.779	14.53	76.49	87.75	84.67	685.77
C	calc min Φ	−	5.832	7.721	14.753	96.238	99.317	93.796	649.33
	calc min G	295	5.888	7.925	14.843	96.175	99.358	93.753	677.04
	exp[1]	295	6.06	7.90	14.88	96.74	100.54	94.20	692.38
	exp[17]	295	6.079	7.893	14.78	96.80	100.08	94.40	689.87

[a] The experimental structures[1−5,17] are compared to the minimum Φ structures for phases **H** and **C**, and to the minimum $G(p,T)$ structures calculated at the same temperature T (K) of the experiments. Unit cell axes a, b, c are in Å, angles α, β, γ in degrees, and cell volumes V in Å^3. Transformations to reduced Niggli cells have been enforced where necessary.

TABLE 2: Raman Frequencies (cm^{-1}) of the Lattice and Intramolecular Modes for Polymorphs C and H of Pentacene at 79 K[a]

polymorph **C**			polymorph **H**			ab initio	
exp	calc	int %	exp	calc	int %	freq	sym
49.4	43.8	1	44.9	26.8	0		
54.9	53.6	3	65.5	60.0	5		
66.9	59.8	8	84.3	68.6	5		
(99.8)	104.5	3	99.1	95.4	14		
140.6	151.3	6	144.1	153.8	25		
147.5	163.1	20	149.5	160.5	14		
126.7	141.2	72	132.2	131.3	89	99.74	b_{1g}
	149.1	91	136.2	146.6	56		
190.8	204.5	97	191.3	202.1	96	146.72	b_{2g}
195.8	206.4	99	196.8	204.4	96		
245.4	235.8	100	247.3	237.5	100	228.45	b_{3g}
	237.7	100		240.1	100		
(269.8)	257.3	100	(270.0)	258.1	100	253.87	a_g
	260.2	100		261.2	100		

[a] We report the experimental A_g frequencies, the corresponding minimum $G(p,T)$ calculations, the percentage of the intramolecular component, and for the intramolecular modes, the ab initio frequency and symmetry of the parent mode in the isolated D_{2h} molecule. Frequencies in parentheses are extrapolated from measurements at higher temperatures.

(QHLD) methods. In this method, where the vibrational Gibbs energy of the phonons is estimated in the harmonic approximation, the Gibbs energy of the system is $G(p,T) = \Phi + pV + \sum_i h\nu_i/2 + k_B T \sum_i \ln[1 - \exp(-h\nu_i/k_B T)]$. Here V is the molar volume, $\sum_i h\nu_i/2$ is the zero-point energy, and the last term is the entropic contribution. The sums are extended to all phonon frequencies ν_i. Because pentacene exhibits ab initio frequencies as low as 38 cm^{-1}, we had to allow for the coupling between lattice and intramolecular vibrations, found to be necessary in similar cases.[23,32] We adopted an exciton-like model,[24,30] where the interaction between different molecular coordinates is mediated by the intermolecular potential which, being a function of the interatomic distance, depends directly on the atomic displacements. Because these correspond to the Cartesian eigenvectors of the normal modes of the isolated molecule, we used the ab initio eigenvectors and the scaled ab initio frequencies. Intramolecular modes above 300 cm^{-1} were not taken into account, because the coupling is important only for low-frequency modes.[13]

Computational Results

Crystallographic Structures. In Table 1, we compare the lattice parameters of all known experimental structures[1−5,17] to the calculated parameters of the structures at the minima of Φ and at the minima of $G(p,T)$. The latter were calculated at ambient pressure, with the same temperatures of the experiments. For the structure of Campbell et al.,[1,2] originally published in a nonstandard crystallographic frame,[4,5] we have applied the usual transformation[33] to the equivalent reduced Niggli cell. The differences between this transformed structure and most other recent structures[3−5] are genuine and do not arise from problems in the older measurements. In fact, as shown in the table, *both* kinds of structures are reproduced by our new X-ray experiments[17] on samples with different morphologies. As previously discussed, the calculations presented in the table yield two distinct potential minima, and thus two distinct phases. The structure of Campbell et al.[1,2] converges to the minimum indicated as **C**, whereas all other published structures[3−5] converge to the minimum indicated as **H**.

Table 1 shows that the minimum Φ structures **C** and **H** reproduce fairly well the experimental lattice parameters of the two corresponding phases, with residual differences ≈3% for the unit cell axes and angles. The most significant shortcoming of the minimum Φ structures is in the unit cell volumes, which are at least 4% smaller than the experimental ones at room temperatures. For the **H** phase, where experiments at several temperatures are available, the volume discrepancy decreases upon cooling, showing that it is partly due to the thermal expansion, totally neglected in the minimum Φ calculations. In fact, as can be seen from the results of the minimum $G(p,T)$ calculations, including vibrational effects brings the calculated volumes within 2% of the experimental ones, or better, and reproduces correctly the thermal expansion of the **H** phase. The experimental volume expansion[5] from 90 to 293 K is 3.5%, to be compared with a calculated value of 2.7%. The coupling between lattice and intramolecular vibrations is important, because the calculated expansion falls down to 1.9% by neglecting it.

For both phases, the QHLD calculations exhibit a mechanical instability for $T > 550$ K, where no minimum of $G(p,T)$ can be found and the crystal structure diverges. Experimental melting temperatures are given as $T \approx 544$ K,[34] or $T \geq 573$ K.[35] As discussed elsewhere,[20,21] loss of mechanical stability in QHLD calculations is not necessarily coincident with melting, but is often close to it. A good agreement is also found for the experimental sublimation heat[36] (unspecified phase) $\Delta_{sub}H = 184 \pm 10$ kJ/mol, which is to be compared with the Gibbs energy calculated[13] at 0 K, $G \approx 174$ kJ/mol for both phases.

Phonon Frequencies. In Figure 2 we compare the experimental Raman frequencies for phases **C** and **H** as a function of

temperature to the corresponding minimum $G(p,T)$ calculations. Lattice and intramolecular modes are both shown. Experimental and calculated Raman frequencies for the two phases at 79 K are summarized in Table 2, where we also report the percentage of the intramolecular component in the eigenvectors. For the intramolecular modes, we indicate the scaled ab initio frequency and the symmetry of the dominant parent mode in the isolated D_{2h} molecule.

The analysis of the eigenvector components in Table 2 justify the choice of neglecting the coupling with the high-frequency intramolecular vibrations, by showing that modes above 200 cm^{-1} are already 100% intramolecular in character. Only some low-frequency modes have a negligible intramolecular contribution, whereas most modes in the intermediate range 60−200 cm^{-1} exhibit a significant mixing, without any recognizable trend. This behavior confirms that the interactions between lattice and intramolecular vibrations are important for pentacene, as expected for this highly flexible molecule, and as predicted by Filippini and Gramaccioli[32] in one of the first systematic studies on this kind of coupling in molecular crystals.

As already found at room temperature,[16] the patterns of calculated frequencies for the lattice modes of phases **C** and **H** at 79 K match the corresponding experimental patterns. In particular, the computations correctly predict the three modes around 55 cm^{-1} plus the mode at 100 cm^{-1} for phase **C**, and the four modes spread below 100 cm^{-1} for phase **H**. The remaining lattice modes are predicted around 140 cm^{-1} for both phases, in agreement with the experiments. Also correct are the predictions for the intramolecular modes, for which all experimental bands agree with the calculations. In fact, once it is considered that only the lower ones of the calculated intramolecular doublets are wide enough to be experimentally resolved, none of the A_g modes predicted for the investigated frequency range remains unaccounted for.

The temperature dependence of the phonon frequencies calculated for phases **C** and **H** (Figure 2), agrees well with the corresponding experimental results. As expected, both experiments and calculations show that varying the temperature affects the low-frequency lattice modes much more than the purely intramolecular modes above 200 cm^{-1}. The modes with mixed intramolecular and lattice character below 200 cm^{-1} exhibit an intermediate behavior.

Discussion and Conclusions

In the present work we have measured the Raman phonon spectra as a function of temperature for lattice and intramolecular modes up to 250 cm^{-1}, for polymorphs **C** and **H** of pentacene. Thanks to the improved spectral resolution at low temperatures, we have been able to assign all Raman active lattice modes, together with all expected intramolecular modes in the frequency range of interest. No discontinuity or change of slope in the Raman frequencies, which might signal a phase transition, has been observed.

By describing the vibrational contribution to the Gibbs energy with quasi harmonic lattice dynamics[19−21,24] (QHLD) methods, we have computed the temperature dependence of the crystal structures and phonon frequencies, and evaluated the effects of the coupling between lattice and intramolecular vibrations. The calculations describe correctly the crystallographic structures[1−5,17] of the polymorphs **C** and **H**. For polymorph **H**, where structures at several temperatures[3−5] are available, we obtain a good agreement with the experimental thermal expansion, especially when the effect of the intramolecular vibrational degrees of freedom is taken into account. The experimental melting temperature[34,35] and sublimation heat[36] are well described by the calculations. The characteristic differences between the patterns of experimental Raman frequencies of the two polymorphs, as well as the corresponding temperature dependence of the frequencies, are also well reproduced. The excellent agreement between experiments and calculations provides a successful stringent test of the QHLD calculations and allows a complete assignment for the observed lattice and intramolecular modes.

The results of this study support the previous analysis on the nature of the pressure induced phase transition.[17,18] This sluggish transition, although not necessarily driven only by the density difference between the structures **C** and **H**, certainly represents a transformation toward the denser structure **H**. One may wonder whether a similar phase transition could also occur at low temperatures. On one hand, because the transition under pressure starts already at 0.2 GPa, contractions even larger than that caused by such a moderate pressure may easily be obtained by cooling. On the other hand, the pressure induced phase transition is quite insensitive to effects of temperature,[17,18] because thermal annealing under pressure does not affect the transition rate, and even cooling to 4.2 K does not trigger any transition. The QHLD calculations confirm that the effects of temperature are not very important. In fact, the computed Gibbs energy difference ΔG between phases **C** and **H**, which would represent the driving force of a possible temperature induced phase transition, is very small at all T. At $T = 300$ K, for example, we find $\Delta G \approx 0.5$ kJ/mol, to be compared with $G \approx 216$ kJ/mol and $k_B T \approx 2.5$ kJ/mol. Furthermore, we have not found any sign change of the computed ΔG, which would indicate a predicted phase transition,[20] in the whole range from 0 K to the melting temperature. The experimental observation that the spectra taken over a wide range of T do not reveal any phase transition, which also indicates that thermal effects are small, is thus not completely unexpected.

References and Notes

(1) Campbell, R. B.; Roberston, J. M.; Trotter, J. *Acta Crystallogr.* **1961**, *14*, 705.

(2) Campbell, R. B.; Roberston, J. M.; Trotter, J. *Acta Crystallogr.* **1962**, *15*, 289.

(3) Holmes, D.; Kumaraswamy, S.; Matzger, A. J.; Vollhardt, K. P. *Chem. Eur. J.* **1999**, *5*, 3399.

(4) Siegrist, T.; Kloc, Ch.; Schön, J. H.; Batlogg, B.; Haddon, R. C.; Berg, S.; Thomas, G. A. *Angew. Chem., Int. Ed. Engl.* **2001**, *40*, 1732.

(5) Mattheus, C. C.; Dros, A. B.; Baas, J.; Meetsma, A.; de Boer, J. L.; Palstra, T. T. M. *Acta Crystallogr. C* **2001**, *57*, 939.

(6) Bouchoms, I. P. M.; Schoonveld, W. A.; Vrijmoeth, J.; Klapwijk, T. M. *Synth. Met.* **1999**, *104*, 175.

(7) Gundlach, D. J.; Jackson, T. N.; Schlom, D. G.; Nelson, S. F. *Appl. Phys. Lett.* **1999**, *74*, 3302.

(8) Lukas, S.; Witte, G.; Wöll, Ch. *Phys. Rev. Lett.* **2002**, *88*, 028301.

(9) Mattheus, C. C.; Dros, A. B.; Baas, J.; Oostergetel, G. T.; Meetsma, A.; de Boer, J. L.; Palstra, T. T. M. *Synth. Met.* **2003**, *138*, 475.

(10) Mattheus, C. C.; de Wijs, G. A.; de Groot, R. A.; Palstra, T. T. M. *J. Am. Chem. Soc.* **2003**, *125*, 6323.

(11) Northrup, J. E.; Tiago, M. L.; Louie, S. G. *Phys. Rev. B* **2003**, *66*, 121404(R).

(12) Venuti, E.; Della Valle, R. G.; Brillante, A.; Masino, M.; Girlando, A. *J. Am. Chem. Soc.* **2002**, *124*, 2128.

(13) Masino, M.; Girlando, A.; Della Valle, R. G.; Venuti, E.; Farina, L.; Brillante, A. *Mater. Res. Soc. Symp. Proc.* **2002**, *725*, 149.

(14) Stillinger, F. H.; Weber, T. A. *Phys. Rev. A* **1982**, *25*, 978.

(15) Della Valle, R. G.; Venuti, E.; Brillante, A.; Girlando, A. *J. Chem. Phys.* **2003**, *118*, 807.

(16) Brillante, A.; Della Valle, R. G.; Farina, L.; Girlando, A.; Masino, M.; Venuti, E. *Chem. Phys. Lett.* **2002**, *357*, 32.

(17) Farina, L.; Brillante, A.; Della Valle, R. G.; Venuti, E.; Amboage, M.; Syassen, K. *Chem. Phys. Lett.* **2003**, *375*, 490.

(18) Farina, L.; Syassen, K.; Brillante, A.; Della Valle, R. G.; Venuti, E.; Karl, N. *High-Pressure Res.* **2003**, *23*, 349; http://www.fci.unibo.it/~valle/.

(19) Ludwig, W. *Recent Developments in Lattice Theory, Springer Tracts in Modern Physics*; Springer-Verlag: Berlin, 1967; Vol. 43.
(20) Della Valle, R. G.; Venuti, E.; Brillante, A. *Chem. Phys.* **1996**, *202*, 231.
(21) Della Valle, R. G.; Venuti, E. *Phys. Rev. B* **1998**, *58*, 206.
(22) Akoi-Matsumoto, T.; Furuta, K.; Yamada, T.; Moriya, H.; Mizuno, K. *Int. J. Mod. Phys. B* **2001**, *15*, 3753.
(23) Della Valle, R. G.; Venuti, E.; Farina, L.; Brillante, A. *Chem. Phys.* **2001**, *273*, 197.
(24) Girlando, A.; Masino, M.; Visentini, G.; Della Valle, R. G.; Brillante, A.; Venuti, E. *Phys. Rev. B* **2000**, *62*, 14476.
(25) Frisch, M. J.; et al. *Gaussian 98*, Revision A.5; Gaussian, Inc.: Pittsburgh, PA, 1998.
(26) Lee, C.; Yang, W.; Parr, R. G. *Phys. Rev. B* **1988**, *37*, 785.
(27) Rauhut, G.; Pulay, P. *J. Phys. Chem.* **1995**, *99*, 3093.
(28) Scott, A. P.; Radom, L. *J. Phys. Chem.* **1996**, *100*, 16502.
(29) Ohno, K. *J. Mol. Spectrosc.* **1979**, *77*, 329.
(30) Califano, S.; Schettino, V.; Neto, N. *Lattice Dynamics of Molecular Crystals*; Springer-Verlag: Berlin, 1981.
(31) Williams, D. E. *J. Chem. Phys.* **1967**, *47*, 4680.
(32) Filippini, G.; Gramaccioli, C. M. *Chem. Phys. Lett.* **1984**, *104*, 50.
(33) Santoro, A.; Mighell, A. D. *Acta Crystallogr. A* **1970**, *26*, 124.
(34) Philippi, E. *Sitzungsber. Akad. Wiss. Wien, Math.−Naturwiss. Kl., Abt.* **1929**, *2B*, 638.
(35) Dabestani, R.; Ivanov, I. N. *Photochem. Photobiol.* **1999**, *70*, 10.
(36) DeKruif, C. G. *J. Chem. Thermodyn.* **1980**, *12*, 243.